

# Survival of quantum effects for observables after decoherence

G.P. Berman,<sup>1</sup> A.R. Bishop,<sup>2</sup> F. Borgonovi,<sup>3,4</sup> and D.A.R. Dalvit<sup>5</sup>

<sup>1</sup>*Theoretical Division and CNLS, MS B213, Los Alamos National Laboratory, Los Alamos, NM 87545*

<sup>2</sup>*Theoretical Division, MS B210, Los Alamos National Laboratory, Los Alamos, NM 87545*

<sup>3</sup>*Dipartimento di Matematica e Fisica, Università Cattolica, via Musei 41, 25121 Brescia, Italy*

<sup>4</sup>*INFN, Unità di Brescia and INFN, Sezione di Pavia, Italy*

<sup>5</sup>*Theoretical Division, MS B213, Los Alamos National Laboratory, Los Alamos, NM 87545*

(Dated: November 12, 2018)

When a quantum nonlinear system is linearly coupled to an infinite bath of harmonic oscillators, quantum coherence of the system is lost on a decoherence time-scale  $\tau_D$ . Nevertheless, quantum effects for observables may still survive environment-induced decoherence, and be observed for times much larger than the decoherence time-scale. In particular, we show that the Ehrenfest time, which characterizes a departure of quantum dynamics for observables from the corresponding classical dynamics, can be observed for a quasi-classical nonlinear oscillator for times  $\tau \gg \tau_D$ . We discuss this observation in relation to recent experiments on quantum nonlinear systems in the quasi-classical region of parameters.

PACS numbers:

In the last few decades there has been extensive theoretical, and more recently experimental, research on the quantum-classical transition. It has been noted that every physical system is, in fact, an open quantum system interacting with its environment. Consequently, the evolution of the reduced density matrix of the system (obtained after tracing over the environmental variables) evolves in such a way that quantum coherent effects are quickly suppressed. This process of environment-induced decoherence has been considered to be an essential ingredient of the quantum-classical transition [1]. On the other hand, despite the huge number of papers on this subject, only few of them deal with quantum nonlinear systems (e.g. [2, 3, 4, 5, 6]).

We consider in this paper the dynamics of a quantum nonlinear oscillator (QNO)

$$\hat{H} = \hbar\omega\hat{a}^\dagger\hat{a} + \mu\hbar^2(\hat{a}^\dagger\hat{a})^2, \quad (1)$$

interacting with a bath of linear oscillators which are initially in thermal equilibrium. Here  $\hat{a}$  ( $\hat{a}^\dagger$ ) are annihilation (creation) bosonic operators,  $\omega$  is the linear frequency and  $\mu$  is the parameter of nonlinearity. The QNO is initially prepared in a coherent state in the quasi-classical region of parameters. In the classical limit ( $\hbar \rightarrow 0$ ,  $\hat{a} \rightarrow \alpha$ ,  $\hat{a}^\dagger \rightarrow \alpha^*$ ,  $|\alpha| \rightarrow \infty$ ,  $\hbar|\alpha|^2 = J$  - an action of the classical linear oscillator) the Hamiltonian (1) becomes  $H_{\text{cl}} = \omega J + \mu J^2$ . In what follows we use the following dimensionless notation:  $\tau = \omega t$ ,  $\bar{\mu} = \hbar\mu/\omega$ ,  $\mu_{\text{cl}} = \mu J/\omega$  and  $\varepsilon = \hbar/J$ . Thus, the quantum parameter  $\bar{\mu}$  can be presented as a product of two parameters, quantum and classical,  $\bar{\mu} = \varepsilon\mu_{\text{cl}}$ . The parameter  $\mu_{\text{cl}}$  characterizes the nonlinearity in the classical system, and can be written as  $\mu_{\text{cl}} = (J/2\omega)(d\omega_{\text{cl}}/dJ)$ , where  $\omega_{\text{cl}} = dH_{\text{cl}}/dJ = \omega + 2\mu J$  is the classical frequency of nonlinear oscillations. The limit  $\mu_{\text{cl}} \ll 1$  corresponds to weak nonlinearity, while  $\mu_{\text{cl}} \geq 1$  corresponds to strong nonlinearity. The parameter  $\varepsilon$  is a quasi-classical parameter. Namely,  $\varepsilon \sim 1$  corresponds to the “pure” quantum system, and  $\varepsilon \ll 1$  corre-

sponds to the quasi-classical limit, which is the subject of this paper.

We study the following problem: What are the parameter conditions for observation of quantum effects on expectation values (observables) in the QNO dynamics. We describe the dynamics for the QNO for observables taking into account five characteristic time-scales which naturally appear in this system. Three of them characterize the time-scales of the QNO evolving under the Hamiltonian dynamics: (i)  $\tau_{\text{cl}} = 2\pi/\omega_{\text{cl}}$  - the period of nonlinear classical oscillations; (ii)  $\tau_E$  - the so-called Ehrenfest time, which indicates the characteristic time-scale at which quantum dynamics for observables starts to depart from the corresponding classical dynamics; (iii)  $\tau_R$  - a quantum recurrence time, which describes the time-scale for quantum recurrences of observables under the Hamiltonian evolution. There are also two characteristic time-scales related to the interaction of the QNO with the thermal bath: (iv)  $\tau_D$  - a decoherence time, which characterizes the decay of the non-diagonal matrix elements of the reduced density matrix in the eigenbasis of the non-interacting Hamiltonian; and (v)  $\tau_\gamma$  - a time-scale of relaxation of quantum observables due to the interaction with the thermal bath. We demonstrate that even if the decoherence time is much smaller than the Ehrenfest time,  $\tau_D \ll \tau_E$ , one can still observe quantum effects for observables. Actually, the important condition for observation of quantum effects related to the Ehrenfest time-scale is  $\tau_E < \tau_\gamma$ , which may be realized in modern experiments in the quasi-classical region of parameters ( $\varepsilon \ll 1$ ). This means that generally the environment-induced decoherence is insufficient for recovering the quantum-classical correspondence for observables in quantum nonlinear systems. This is an important observation for at least two reasons: (a) It means that pure quantum effects can be observed for times much longer than  $\tau_D$  and (b) Pure quantum dynamical effects can be important in experiments even in

the quasi-classical region of parameters. Finally, the classical limit appears in our system under very natural conditions:  $\tau_D \ll \tau_{cl} \ll \tau_\gamma \ll \tau_E \ll \tau_R$ .

One type of systems that could be considered for observing quantum effects in the quasi-classical region of parameters are Bose-Einstein condensates (BECs). These are particularly suited to analyzing the interplay between nonlinear dynamics and environmental interactions in the realm of quantum mesoscopic systems. This is because they are macroscopic matter waves, often described theoretically by the Gross-Pitaevskii (GP) equation, which formally is a classical nonlinear field-theory. Going beyond GP allows one to understand the role of quantum effects in the quasi-classical region of parameters. Another important feature of BECs is that they are experimentally easily accessible and controllable by means of trapping potentials and tunable interactions. BECs have already been used to demonstrate nonlinear dynamics of collapses and revivals of a coherent matter wave in the pure quantum regime [7]. Here, the condensate was initially trapped in the lowest energy band of a three-dimensional optical lattice. By adiabatically raising the heights of the barriers it was possible to suppress tunneling between sites and at the same time maintain the system in the superfluid regime, so that within each lattice site independent coherent states were engineered with an average number of atoms of order one. Every BEC in each lattice site is well described in the single-mode approximation by the QNO Hamiltonian given in Eq. (1), with  $\omega$  being the trapping frequency in each lattice site and  $\mu$  being proportional to the s-wave two-body scattering length. Other systems that could be used for observation of quantum nonlinear effects in the quasi-classical region of parameters are micro- [9] and nanomechanical [10] resonators, high-frequency cantilevers [11], nonlinear optical systems and superconductive junctions.

The QNO is one of the simplest quantum nonlinear systems for which the breakdown of the quantum-classical correspondence can be exactly calculated. The quantum and classical dynamics of an initial coherent wave packet evolving under Eq. (1) were computed by Berman *et al* [8] and by Milburn [3]. The characteristic time-scale for departure of the quantum dynamics from the corresponding classical one, the so-called Ehrenfest time, was introduced for this system in [8]. In [3] a similar problem was studied using the  $Q$  quasi-probability distribution. It was shown that the presence of non-positive definite second-order terms in the quantum evolution equation for  $Q$ , not present in the evolution of the classical probability density, are responsible for quantum recurrences and prevent the appearance of fine-scale-structure “whorls” predicted in the classical description. In [4, 5] the interaction of the QNO with the environment (modeled by a thermal bath of harmonic oscillators) was studied in the limit of small nonlinearity, and it was argued that such interaction was effective in destroying quantum interference effects and restoring the classical phase-space structure. However, as we already stated, environment-induced decoherence

is in fact ineffective in recovering the quantum-classical correspondence for this nonlinear system.

In the following we compute quantum observables in the coherent state basis. For an arbitrary operator function  $\hat{f} = \hat{f}(\hat{a}^\dagger, \hat{a})$ , the time-dependent expectation value of such a function (observable),  $f(\alpha^*, \alpha, t) = \langle \alpha | e^{i\hat{H}t/\hbar} \hat{f} e^{-i\hat{H}t/\hbar} | \alpha \rangle$ , for an initial coherent state,  $|\alpha\rangle$ , satisfies a partial differential equation of the form [12]:  $\partial f / \partial \tau = \hat{K} f$ , where  $\hat{K} = \hat{K}_{cl} + \hbar \hat{K}_q$ . Here the operator  $\hat{K}_{cl}$  includes only the first order derivatives and describes the corresponding classical limit, while the other operator  $\hat{K}_q$  includes higher order derivatives and is responsible for quantum effects. For the model given by Eq. (1) we get

$$\begin{aligned} \frac{\partial f}{\partial \tau} = & i(1 + \bar{\mu} + 2\bar{\mu}|\alpha|^2) \left( \alpha^* \frac{\partial}{\partial \alpha^*} - \alpha \frac{\partial}{\partial \alpha} \right) f + \\ & i\bar{\mu} \left( (\alpha^*)^2 \frac{\partial^2}{\partial (\alpha^*)^2} - \alpha^2 \frac{\partial^2}{\partial \alpha^2} \right) f. \end{aligned} \quad (2)$$

In particular, for  $\hat{f} = \hat{a}$  the evolution of  $f(\tau)$  corresponds to the evolution of the condensate matter-wave field  $\alpha(\tau) \equiv \langle \alpha | \hat{a}(\tau) | \alpha \rangle$ . In this case Eq. (2) can be solved exactly [12]:

$$\alpha(\tau) = \alpha e^{-i(1+\bar{\mu})\tau} \exp[|\alpha|^2(e^{-2i\bar{\mu}\tau} - 1)]. \quad (3)$$

The quantum evolution of this expectation value departs from the corresponding classical evolution  $\alpha_{cl}(\tau) = \alpha e^{-i\omega_{cl}\tau}$  as  $\alpha(\tau) = \alpha_{cl}(\tau) e^{-\tau^2/2\tau_E^2} [1 + O(\bar{\mu}\tau) + O(|\alpha|^2 \bar{\mu}^3 \tau^3)]$ , where  $\tau_E$  is the Ehrenfest time-scale given by

$$\tau_E = \frac{1}{2\bar{\mu}|\alpha|}. \quad (4)$$

The amplitudes of quantum and classical observables coincide at times multiple of the quantum recurrence time-scale

$$\tau_R = \frac{\pi}{\bar{\mu}}. \quad (5)$$

Note that the quasi-classical limit, which is considered in this paper, corresponds to the following condition:  $\tau_E/\tau_R = \varepsilon^{1/2}/2\pi \ll 1$ . So, in what follows we will be interested only in the region of parameters where  $\tau_E \ll \tau_R$ . Quantum recurrences of the matter wave field of a BEC in the *pure* quantum regime  $\alpha \approx O(1)$  (or  $\varepsilon \approx 1$ ) in each lattice site were observed in [7] at  $\tau_R \approx 100$  ( $t_R = 0.55\text{ms}$ ), larger than the corresponding Ehrenfest time-scale  $\tau_E \approx 15$ . At the same time, quantum dynamical effects in the quasi-classical region of parameters have still not been observed in BECs.

Expressing  $\alpha = \sqrt{J/\hbar} e^{-i\theta}$ , we can rewrite Eq. (2) as

$$\frac{\partial f}{\partial \tau} = (1 + 2\mu_{cl}) \frac{\partial f}{\partial \theta} + 2\varepsilon\mu_{cl} \frac{\partial^2 f}{\partial J \partial \theta}. \quad (6)$$

The quantum term appears as a singular perturbation of the classical equation because the small parameter

$\varepsilon$  multiplies the higher order derivative. Note that the quantum effects for observables vanish in two cases: (i)  $\varepsilon = 0$ , which corresponds to the classical limit, and (ii)  $\mu_{\text{cl}} = 0$ , which corresponds to the quantum linear oscillator. The fact that for nonlinear quantum systems the terms with high order derivatives in the evolution equations for the density matrix and for the Wigner function represent a singular perturbation to the classical limit (Liouville function) is well-known. However, in spite of a large number of papers on this subject, from this fact it is still unclear what are the conditions for the quantum-classical correspondence for *observables*. The solution (3) of Eq. (2) for the observable  $\alpha(\tau)$  (and also for an arbitrary observable [12]) demonstrates that quantum effects (second order derivatives in Eqs. (2,6)) represent a singular perturbation to the classical equation for *observables*, which includes only the first order derivatives and can be solved by the method of classical characteristics [8, 12]. This results in a secular behavior of quantum corrections in the solution for the observable  $\alpha(\tau)$  (3). So, the question is: Under what conditions does the environment “kill” (if at all) the quantum corrections which represent a singular perturbation to the *observables* of the classical world?

Following [4, 5] we model the environment as a bath of harmonic oscillators in thermal equilibrium at a rescaled temperature  $\bar{\beta} = \hbar\omega/k_{\text{B}}T$  linearly coupled through position to the QNO [13]. In the Born-Markov approximation, the master equation for the reduced density matrix reads

$$\frac{d\hat{\rho}}{d\tau} = F_{\text{free}}(\hat{\rho}) + F_{\eta}(\hat{\rho}) + F_{\nu}(\hat{\rho}), \quad (7)$$

where the first term,

$$F_{\text{free}}(\hat{\rho}) = -i[\hat{a}^{\dagger}\hat{a} + \bar{\mu}(\hat{a}^{\dagger}\hat{a})^2, \hat{\rho}], \quad (8)$$

corresponds to the free, unitary evolution, the second one

$$F_{\eta}(\hat{\rho}) = \frac{i}{2}[\hat{a} + \hat{a}^{\dagger}, \{\hat{A}_1(\tau)\hat{a} + \hat{a}^{\dagger}\hat{A}_1(\tau) + i(\hat{A}_2(\tau)\hat{a} - \hat{a}^{\dagger}\hat{A}_2(\tau)), \hat{\rho}\}], \quad (9)$$

accounts for dissipation, and the third one,

$$F_{\nu}(\hat{\rho}) = -\frac{1}{2}[\hat{a} + \hat{a}^{\dagger}, [\hat{B}_1(\tau)\hat{a} + \hat{a}^{\dagger}\hat{B}_1(\tau) + i(\hat{B}_2(\tau)\hat{a} - \hat{a}^{\dagger}\hat{B}_2(\tau)), \hat{\rho}]], \quad (10)$$

is related to noise. The time-dependent, operator-valued coefficients  $\hat{A}_i$  and  $\hat{B}_i$  depend on the frequency operator

$$\hat{\Omega} = 1 + \bar{\mu}(1 + 2\hat{a}^{\dagger}\hat{a}),$$

and on the spectral density of the environment

$$J(\bar{\omega}) = \frac{\gamma\bar{\omega}\bar{\Lambda}^2}{\bar{\Lambda}^2 + \bar{\omega}^2},$$

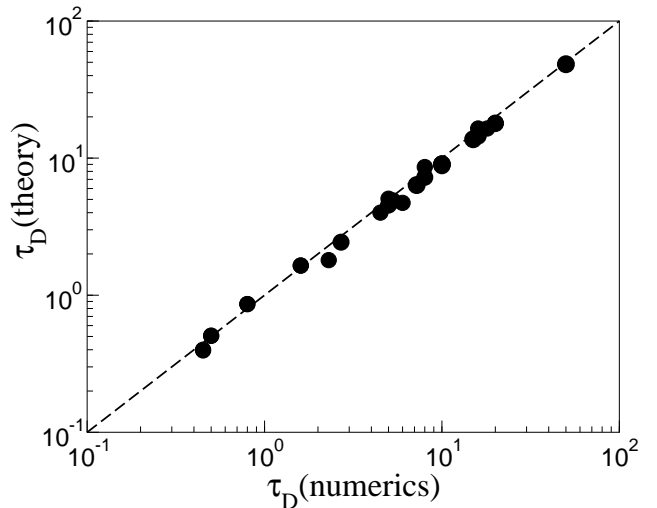


FIG. 1: Comparison between the numerically obtained decoherence time  $\tau_D$  and the approximate relation given by Eq. (19), obtained retaining only one term in the master equation. The dashed line corresponds to  $\tau_D(\text{theory}) = \tau_D(\text{numerics})$ . Data are obtained by varying parameters in the following regions:  $20 \leq I_0 \leq 100$ ,  $10^{-3} \leq \bar{\mu} \leq 4$ ,  $10^{-2} \leq \bar{\beta} \leq 1$ ,  $10^{-5} \leq \gamma \leq 10^{-2}$ .

that we chose to be Ohmic, with  $\bar{\Lambda}$  a UV cut-off and  $\gamma$  a system-environment coupling constant. Explicitly

$$\hat{A}_1(\tau) = \int_0^\tau ds \eta(s) \cos(\hat{\Omega}s); \quad (11)$$

$$\hat{A}_2(\tau) = \int_0^\tau ds \eta(s) \sin(\hat{\Omega}s); \quad (12)$$

$$\hat{B}_1(\tau) = \int_0^\tau ds \nu(s) \cos(\hat{\Omega}s); \quad (13)$$

$$\hat{B}_2(\tau) = \int_0^\tau ds \nu(s) \sin(\hat{\Omega}s), \quad (14)$$

where the dissipation and noise kernels are respectively given by

$$\eta(s) = \int_0^\infty d\bar{\omega} \frac{\bar{\omega}}{\pi} J(\bar{\omega}) \sin(\bar{\omega}s); \quad (15)$$

$$\nu(s) = \int_0^\infty d\bar{\omega} \frac{\bar{\omega}}{\pi} J(\bar{\omega}) \coth\left(\frac{\bar{\beta}\bar{\omega}}{2}\right) \cos(\bar{\omega}s). \quad (16)$$

The matrix elements of the operators  $\hat{A}_i$  and  $\hat{B}_i$  can be straightforwardly computed in the Fock basis and shown to have an analogous behavior to that of the  $\bar{\mu} = 0$ , quantum Brownian motion case [14].

To study the decoherence effects of the environment we start by considering an initial Schrödinger cat state formed by large-amplitude coherent states,  $\hat{\rho}(0) = \mathcal{N}(|\alpha\rangle + |\beta\rangle)(\langle\alpha| + \langle\beta|)$ , with  $|\alpha|^2, |\beta|^2 \gg 1$ , and  $\mathcal{N}$  a normalization constant. For simplicity we take  $\alpha$  and  $\beta$  to lie along a common radius, and we parameterize them as  $\alpha = xe^{i\theta}$  and  $\beta = (x + \delta x)e^{i\theta}$ . Decoherence is due to the term in the master equation containing  $\hat{B}_1$ . In the

coherent state basis, the off-diagonal matrix elements of the density matrix evolve as

$$\frac{d}{d\tau} \langle \alpha | \hat{\rho} | \beta \rangle \approx -2B_1(I_0, \tau) (\delta x)^2 \langle \alpha | \hat{\rho} | \beta \rangle, \quad (17)$$

where  $B_1(I_0, \tau) = \langle \alpha | \hat{B}_1(\tau) | \alpha \rangle$  with  $I_0 \equiv |\alpha|^2$ . For  $\tau \gg 1/\bar{\Lambda}$ ,  $B_1(I_0, \tau)$  is approximately equal to its asymptotic value

$$B_1(I_0, \infty) = \frac{\gamma \bar{\Omega}}{2} \frac{\bar{\Lambda}^2}{\bar{\Lambda}^2 + \bar{\Omega}^2} \coth\left(\frac{\bar{\beta} \bar{\Omega}}{2}\right),$$

with  $\bar{\Omega} = 1 + \bar{\mu}(1 + 2I_0)$ . Therefore, the decoherence time-scale is

$$\tau_D = \frac{1}{2B_1(\infty)(\delta x)^2}. \quad (18)$$

This decoherence time-scale coincides with the time-scale for exponential decay of quantum recurrences for an initial coherent state  $|\alpha\rangle$  coupled to the thermal bath. Indeed, in this case  $(\delta x)^2 \approx \langle \alpha | x^2 | \alpha \rangle \approx I_0$ , so that

$$\tau_D = \frac{\tanh(\bar{\beta} \bar{\Omega} / 2)}{I_0 \gamma \bar{\Omega}}. \quad (19)$$

We checked this estimation by numerical simulations of Eq. (7) using as initial state a quasi-classical coherent state. As can be seen in Fig. 1, the agreement is fairly good within the numerical errors. In the limit of small temperature  $\bar{\beta} \bar{\Omega} \gg 1$  and small non-linearity  $\bar{\mu} I_0 \ll 1$  the decoherence time-scale coincides with the one derived in [4]; however, we stress that in the general case, differently from [4], the decoherence time, as given by (19), depends on the parameter of nonlinearity  $\bar{\mu}$ . In the high-temperature limit,  $\bar{\beta} \bar{\Omega} \ll 1$ , the decoherence time is:  $\tau_D \approx \tau_\gamma \hbar^2 \omega / 4k_B T J_{\text{cl}}$ , where  $\tau_\gamma = 2/\gamma$  is the time scale of the relaxation of quantum observables due to the interaction with the environment.

Having the density matrix elements, we can easily determine the average values of any observable, for instance, for the position  $x(\tau) \equiv \langle \hat{x}(\tau) \rangle = (\alpha(\tau) + \alpha^*(\tau))/\sqrt{2}$ . An example of such simulations is given in Fig. 2. The time-scale for the overall decay of the amplitude of recurrences, shown in Fig. 2a, is set by the decoherence time-scale  $\tau_D$ : the relative heights of two peaks, taken at two neighbor recurrent times, is reduced by a factor  $\exp(-\tau_R/\tau_D)$ . An enlargement of the first bump of Fig. 2a is given in Fig. 2b. As one can see in both cases reported in the figure, the time-scale which governs the envelope of  $x(\tau)$  is the Ehrenfest time  $\tau_E$ , which is independent of the coupling to the environment. The same is true for any of the following revival bumps, see Fig. 2c. Let us also notice that in Fig. 2b the curves for  $\gamma = 10^{-4}$  (solid line) and for  $\gamma = 10^{-2}$  (dashed-dotted line) are slightly shifted one to the other. This is due to the fact that the frequency of motion is slightly dependent on the bath-oscillator interaction strength,  $\omega_{\text{eff}}^2 = \bar{\Omega}^2 - \gamma \bar{\Lambda}^3 / (\bar{\Lambda}^2 + \bar{\Omega}^2)$ . This is not at all

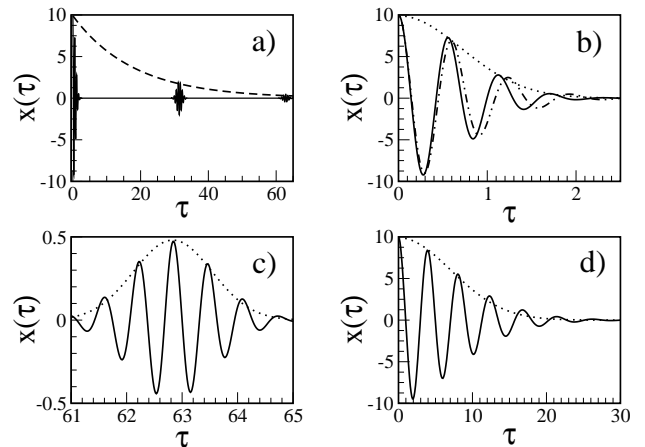


FIG. 2: The average position as a function of the dimensionless time  $\tau$ . In all cases  $I_0 = 50$ ,  $\bar{\beta} = 1$ . a) Parameters are  $\bar{\mu} = 0.1$  and  $\gamma = 10^{-4}$ . The dashed curve corresponds to  $\exp(-\tau/\tau_D)$ , where  $\tau_D = 18 > \tau_E \approx 0.7$ . b) is an enlargement of the first bump of a). Two more curves have been added: a dashed-dotted line corresponds to the average position for  $\gamma = 10^{-2}$ , so that  $\tau_D = 0.18 < \tau_E$ ; and a dotted line that corresponds to the envelope  $\exp(-\tau^2/2\tau_E^2)$ . c) is an enlargement of the third bump of a). The dotted line corresponds to the envelope  $\exp(-\tau_R/\tau_D) \exp[-(\tau - \tau_R)^2/2\tau_E^2]$ , where  $\tau_R = 10\pi$ . d) Parameters are  $\bar{\mu} = \gamma = 10^{-2}$ , so that  $\tau_D \ll \tau_E \ll \tau_\gamma < \tau_R$ .

surprising since the renormalization of the frequency is a feature of the considered master equation [14].

In Fig. 2d the average position is plotted for a case in which  $\tau_D \ll \tau_E \ll \tau_\gamma < \tau_R$  ( $\tau_D = 0.74$ ,  $\tau_{\text{cl}} = 3.12$ ,  $\tau_E = 7.1$ ,  $\tau_\gamma = 200$  and  $\tau_R = 314$ ). This figure represents the most important result of the present work: Usually, in the quasi-classical region of parameters, and for rather large values of the coupling to the environment ( $\gamma \geq 10^{-2}$ ), the characteristic decoherence time-scale is much shorter than the Ehrenfest time scale,  $\tau_D \ll \tau_E$ . Despite this, the system does not become entirely “classical”, since quantum effects persist up to the Ehrenfest time. Indeed, for  $x(0) = (\alpha + \alpha^*)/\sqrt{2} = \sqrt{2I_0} = 10$  and  $\tau_D = 0.74$ , the dependence  $x(0) \exp(-\tau/\tau_D)$  would give us, for example, for  $\tau = 10$  the value  $1.3 \times 10^{-5}$ , which is significantly smaller than the correspondent value 3.7 defined by the function  $x(0) \exp(-\tau^2/2\tau_E^2)$  for  $x(0) = 10$ ,  $\tau = 10$  and  $\tau_E = 7.1$  (which corresponds to the results presented in Fig. 2d.)

In our model the classical limit corresponds to the following inequalities:  $\tau_D \ll \tau_{\text{cl}} \ll \tau_\gamma \ll \tau_E \ll \tau_R$  (see Fig. 3). Because in the quasi-classical region of parameters the inequalities  $\tau_E \ll \tau_R$  and  $\tau_D \ll \tau_{\text{cl}}$  are always satisfied, the really important condition for the classical limit is  $\tau_\gamma \ll \tau_E$ . In this case the system effectively behaves as a classical damped oscillator, and quantum effects cannot be observed. For comparison we plot in Fig. 3 the overall decay of oscillation, given by  $\tau_\gamma$ , with the one that would be given by the Ehrenfest time. The perfect agreement of the decay relaxation time with the data and their wrong

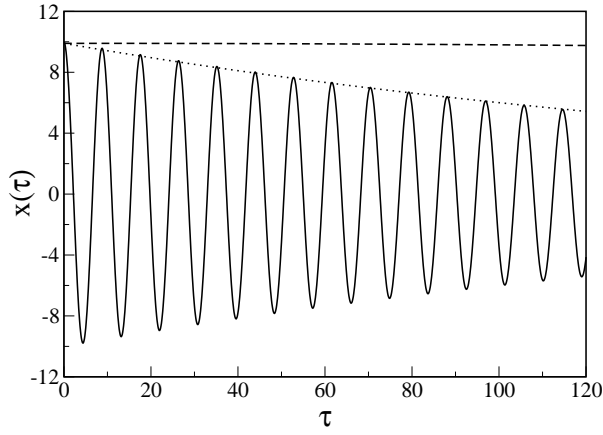


FIG. 3: The average position  $x(\tau)$  in the “classical” limit:  $\tau_D \ll \tau_{cl} \ll \tau_\gamma \ll \tau_E \ll \tau_R$ . Parameters are:  $\bar{\mu} = 10^{-4}$ ,  $\bar{\beta} = 1$ ,  $\gamma = 0.01$ ,  $I_0 = 50$ , so that  $\tau_D = 0.92$ ,  $\tau_{cl} = 2\pi$ ,  $\tau_\gamma = 200$ ,  $\tau_E = 707$ ,  $\tau_R = \pi \times 10^4$ . The correct decay (dotted line), as given by the relaxation time  $\tau_\gamma$ , is compared with the “wrong” decay (dashed line) given by the Ehrenfest time  $\tau_E$ .

dependence on the Ehrenfest time is a manifestation of the classicality for this case.

To gain a qualitative understanding of these numerical findings we consider a simplified version of our master equation Eq. (7) at zero temperature, in which we keep only the effect of dissipation and decoherence due to the environment, and make the rotating wave approximation. In this way we get the standard master equation in quantum optics for the QNO:

$$\frac{d\hat{\rho}}{d\tau} = -i[\hat{a}^\dagger\hat{a} + \bar{\mu}(\hat{a}^\dagger\hat{a})^2, \hat{\rho}] + \frac{\gamma}{2}(2\hat{a}\hat{\rho}\hat{a}^\dagger - \hat{a}^\dagger\hat{a}\hat{\rho} - \hat{\rho}\hat{a}^\dagger\hat{a}). \quad (20)$$

This equation is precisely the one considered in [4], where an exact solution for the quasi-probability  $Q$  function was obtained, assuming an initial coherent state  $|\alpha\rangle$ . In particular, an exact expression for time-evolution of the average position  $\langle \hat{x}(\tau) \rangle = (\langle \hat{a}(\tau) \rangle + \langle \hat{a}^\dagger(\tau) \rangle)/\sqrt{2}$  can be written, where

$$\langle \hat{a}(\tau) \rangle = \alpha e^{(1+\bar{\mu})\tau} e^{-\frac{\gamma\tau}{2}} e^{-\frac{1+\bar{\mu}}{1+k^2}(1+ik)(1-e^{-\gamma\tau})e^{-2i\bar{\mu}\tau}}, \quad (21)$$

with  $k = \gamma/2\bar{\mu}$ . Note that for no coupling to the environment ( $\gamma = 0$ ) we recover Eq. (3). From Eq. (21) we can read the decay factor of the average position  $x(\tau) \propto e^{-D(\tau)}$ . It is given by

$$D(\tau) = \frac{\gamma\tau}{2} + \frac{4\bar{\mu}^2|\alpha|^2}{4\bar{\mu}^2 + \gamma^2} \times \left[ (1 - e^{-\gamma\tau} \cos(2\bar{\mu}\tau)) - \frac{\gamma}{2\bar{\mu}} e^{-\gamma\tau} \sin(2\bar{\mu}\tau) \right]. \quad (22)$$

Let us first analyze the case  $\gamma/2 \ll \bar{\mu}$ , corresponding to  $\tau_E \ll \tau_\gamma$ . Let us express the time  $\tau$  around a given recurrence time as  $\tau = n\tau_R + \tilde{\tau}$ , where  $n$  is a non-negative integer. Assuming that the time  $\tau$  is much shorter than

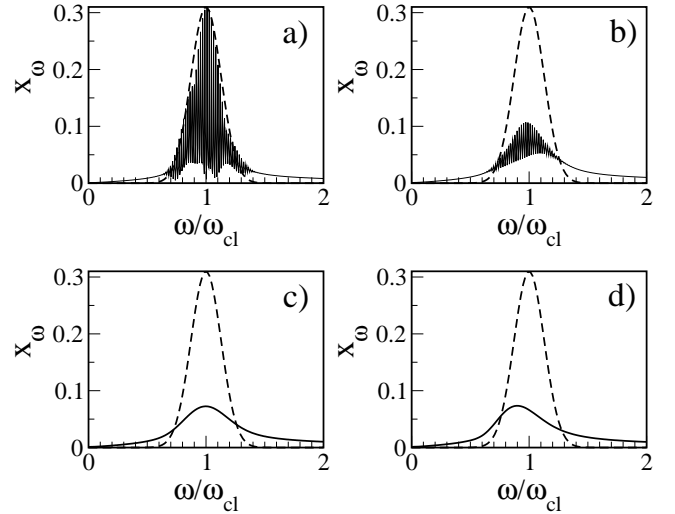


FIG. 4: The Fourier spectrum of the average position versus the rescaled frequency, where  $\omega_{cl} = 1 + 2\bar{\mu}I_0$  is the classical frequency. As the dashed black line we show the theoretical expression Eq. (25) for the closed system. Parameters  $\bar{\beta}, \bar{\mu}, I_0$  are the same as in Fig. (2), while a)  $\gamma = 10^{-5}$ ,  $\tau_D = 180 \gg \tau_E = 0.7$ , b)  $\gamma = 10^{-4}$ ,  $\tau_D = 18 > \tau_E = 0.7$  c)  $\gamma = 10^{-3}$ ,  $\tau_D = 1.8 > \tau_E = 0.7$  d)  $\gamma = 10^{-2}$ ,  $\tau_D = 0.18 < \tau_E = 0.7$  As one can see, decreasing of the decoherence time has no effects on the width of the Fourier spectrum.

the relaxation time,  $\gamma\tau \ll 1$ , and that  $\bar{\mu}\tilde{\tau} \ll 1$ , we can expand  $D(\tau) \approx |\alpha|^2(2\bar{\mu}^2\tilde{\tau}^2 + n\tau_R\gamma)$ . Hence, in these limits, the decay of the average position is

$$x(\tau) \propto e^{-\tilde{\tau}^2/2\tau_E^2} e^{-n\tau_R/\tau_D}, \quad (23)$$

where  $\tau_E$  is defined in Eq. (4) and  $\tau_D = 1/\gamma|\alpha|^2$  is the zero temperature limit of Eq. (19) for  $\bar{\mu}|\alpha|^2 \ll 1$ . Therefore, the decay of  $x(\tau)$  within any recurrence bump is determined by the Ehrenfest time-scale, and even in the limit  $\tau_D \ll \tau_E$  the decay within the first bump ( $n = 0$ ) is still governed by the Ehrenfest time-scale, which agrees with our numerical results presented above. This implies that some quantum effects survive the loss of quantum coherence due to the interaction with the environment. One the other hand, when  $\gamma/2 \gg \bar{\mu}$  (i.e.,  $\tau_\gamma \ll \tau_E$ ) the classical limit is attained, and the decay is governed by the relaxation rate.

Persistence of quantum effects after the decoherence time can be also observed analyzing the Fourier spectrum of the average position in time  $x(\tau) = \sum_\omega x_\omega e^{i\omega\tau}$ . When the system is closed, i.e. no coupling to the environment, the Fourier components are given by

$$x_\omega = \frac{\alpha}{2} \Lambda \left( \frac{\omega - 1}{2\bar{\mu}} \right) + \text{c.c.},$$

where

$$\Lambda(n) = \frac{\bar{\mu}}{\pi} \int_0^{\pi/\bar{\mu}} e^{(e^{2i\bar{\mu}\tau} - 1)|\alpha|^2 - 2i\bar{\mu}n\tau} d\tau. \quad (24)$$

Estimating this quantity in the limit  $\bar{\mu}\tau \ll 1$  we obtain the frequency spectrum for the QNO,

$$x_\omega \approx \frac{1}{\sqrt{4\pi|\alpha|^2}} \exp\left[-\frac{(\omega - \omega_{\text{cl}})^2}{2\Delta\omega^2}\right] x(0), \quad (25)$$

which is a Gaussian distribution centered around the classical oscillation frequency  $\omega_{\text{cl}} = 1 + 2\bar{\mu}|\alpha|^2$  with a spectral width given by the inverse of the Ehrenfest time-scale,  $\Delta\omega = \tau_E^{-1}$ . In Fig. 4 the Fourier spectrum  $x_\omega$  for the QNO coupled to the environment is shown for the case  $\tau_E \ll \tau_\gamma$ . As one can see, in all cases presented in Fig. 4 (whatever the relation is between the decoherence time and the Ehrenfest time) the width of the Fourier spectrum is always given by the inverse Ehrenfest time. When  $\tau_\gamma \ll \tau_E$  the width of the spectrum is given by the relaxation rate, and the classical limit is obtained.

The important condition for survival of the quantum effects for observables related to the Ehrenfest time-scale is  $\tau_E \ll \tau_\gamma$ , which can be written in the form

$$\Theta \equiv \frac{\tau_\gamma}{\tau_E} = 2\mu_{\text{cl}}\varepsilon^{1/2}\tau_\gamma \gg 1. \quad (26)$$

For BECs the parameter of nonlinearity  $\mu_{\text{cl}} = \mu J/\omega$  can be written as  $\mu_{\text{cl}} = N\sqrt{a^2 m\omega/2\pi\hbar}$ , where  $N$  is the number of particles in the condensate,  $a$  is the s-wave scattering length,  $m$  is the mass of the atoms and  $\omega$  is the trapping frequency. The quasi-classical parameter is  $\varepsilon = 1/N$ . Therefore

$$\Theta_{\text{BEC}} = a\sqrt{\frac{2m\omega N}{\pi\hbar}}\tau_\gamma \gg 1. \quad (27)$$

For example, for  $a = 5\text{nm}$ ,  $m = 1.5 \times 10^{-25}\text{kg}$ ,  $\omega/2\pi = 100\text{Hz}$  and estimating the dimensionless relaxation time  $\tau_\gamma$  from the lifetime of the condensate (say  $t_\gamma = 1\text{sec}$ , so  $\tau_\gamma = \omega t_\gamma = 2\pi \times 10^2$ ), we need a total number of particles  $N \gg 1$ . In the case of a cantilever (or a mechanical resonator) the quasi-classical parameter is  $\varepsilon = 1/n$ , where  $n$  is the average number of levels involved in the coherent state of the cantilever. For the dimensionless relaxation time  $\tau_\gamma$  we take  $\tau_\gamma = 2Q$ , where  $Q$  is the cantilever quality factor. Then, for a cantilever the condition (26) takes the form

$$\Theta_{\text{cantilever}} = \frac{4\mu_{\text{cl}}Q}{\sqrt{n}} \gg 1. \quad (28)$$

We take the following dimensional parameters [15]: the amplitude of the cantilever oscillations  $x_m = 10\text{nm}$ , the spring constant  $k_c = 6 \times 10^{-4}\text{N/m}$  and the frequency of the fundamental mode of the cantilever  $\omega_c/2\pi = 6.6\text{kHz}$ . In this case, the number of cantilever levels can be estimated as  $n \approx k_c x_m^2/\hbar\omega_c \approx 6 \times 10^{11}$ . We also take  $Q = 10^6$ . Then, we have from Eq. (28) the estimate for the parameter of nonlinearity:  $\mu_{\text{cl}} \gg 0.2$ . We hope that these conditions can be experimentally realized, and quantum effects related to the Ehrenfest time-scale can be observed in the quasi-classical region of parameters.

We acknowledge useful discussions with G. Nardelli. This work was supported by the Department of Energy (DOE) under Contract No. W-7405-ENG-36, and by the Defense Advanced Research Projects Agency (DARPA).

- 
- [1] D. Giulini *et al.*: *Decoherence and the Appearance of a Classical World in Quantum Theory* (Springer, Berlin 1996); W.H. Zurek, *Rev. Mod. Phys.* **75**, 715 (2003).
- [2] F. Haake, H. Risken, C. Savage and D. Walls, *Phys. Rev. A* **34** 3969, (1986).
- [3] G.J. Milburn, *Phys. Rev. A* **33**, 674 (1986).
- [4] G.J. Milburn and C.A. Holmes, *Phys. Rev. Lett.* **56**, 2237 (1986).
- [5] D.J. Daniel and G.J. Milburn, *Phys. Rev. A* **39**, 4628 (1989).
- [6] W.H. Zurek and J.P. Paz, *Phys. Rev. Lett.* **72**, 2508 (1994).
- [7] M. Greiner, O. Mandel, T.W. Hänsch and I. Bloch, *Nature* **419**, 51 (2002).
- [8] G.P. Berman, A.M. Iomin and G.M. Zaslavsky, *Physica D* **4**, 113 (1981).
- [9] H.B. Chan *et al.*, *Phys. Rev. Lett.* **87**, 211801 (2001).
- [10] A.N. Cleland, M.L. Roukes, *J. Appl. Phys.* **92**, 2758 (2002).
- [11] B.C. Stipe *et al.*, *Phys. Rev. Lett.* **87**, 096801 (2001).
- [12] G.P. Berman, E.N. Bulgakov and D.D. Holm, *Crossover-Time in Quantum Boson and Spin Systems* (Springer-Verlag, Berlin, 1994).
- [13] More realistic models for the interaction between the condensate and the environment can be considered. See D.A.R. Dalvit, J. Dziarmaga and W.H. Zurek, *Phys. Rev. A* **62**, 013607 (2000); *Acta Phys. Pol B* **31**, 3065 (2000); e-print cond-mat/0006349.
- [14] J.P. Paz and W.H. Zurek, in *Coherent matter waves, Les Houches Session LXXII*, R. Kaiser, C. Westbrook and F. David eds., EDP Sciences (Springer Verlag, Berlin, 2001) 533-614.
- [15] H.J. Mamin *et al.*, *Phys. Rev. Lett.*, to be published.